CHAPTER IV

RESULTS AND DISCUSSION

4.1 Preparation of 1-Phenylethanol Derivatives

Most of 1-phenylethanol derivatives used in this study were prepared by reduction of their corresponding ketones using sodium borohydride as reducing agent. The products were characterized by NMR spectrometer. The yield of all synthesized alcohols was greater than 80%. However, the preparation of hydroxy-substituted derivatives of 1-phenylethanol was unsuccessful. The structures and abbreviations of compounds to be examined are shown in table 4.1.

Table 4.1 Structures of all 1-phenylethanol derivatives used in this study.

abbreviation	structure	compound name
H	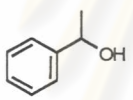	1-phenylethanol
2F	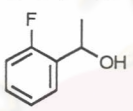	2-fluoro-α-methylbenzyl alcohol
3F	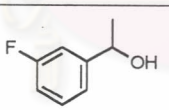	3-fluoro-α-methylbenzyl alcohol
4F	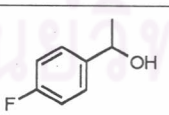	4-fluoro-α-methylbenzyl alcohol
2Cl	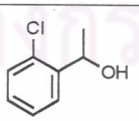	1-(2-chlorophenyl)ethanol
3Cl	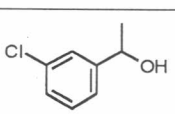	1-(3-chlorophenyl)ethanol
4Cl	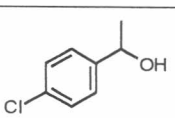	1-(4-chlorophenyl)ethanol

abbreviation	structure	compound name
2Br	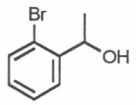	2-bromo-α-methylbenzyl alcohol
3Br	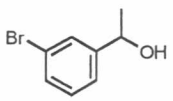	3-bromo-α-methylbenzyl alcohol
4Br	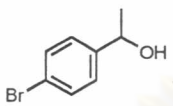	4-bromo-α-methylbenzyl alcohol
2Me	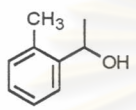	2-methyl-α-methylbenzyl alcohol
3Me	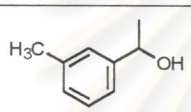	3-methyl-α-methylbenzyl alcohol
4Me	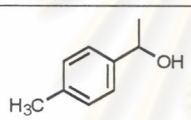	4-methyl-α-methylbenzyl alcohol
2OMe	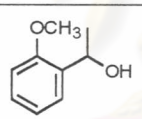	2-methoxy-α-methylbenzyl alcohol
3OMe	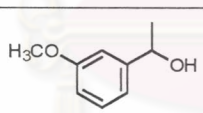	3-methoxy-α-methylbenzyl alcohol
4OMe	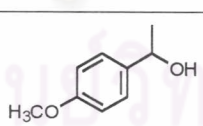	4-methoxy-α-methylbenzyl alcohol
2N	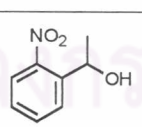	2-nitro-α-methylbenzyl alcohol
3N	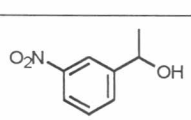	3-nitro-α-methylbenzyl alcohol
4N	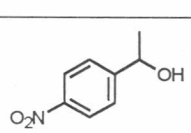	4-nitro-α-methylbenzyl alcohol

abbreviation	structure	compound name
3CN	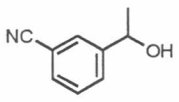	3-cyano-α-methylbenzyl alcohol
4CN	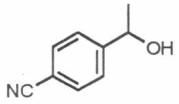	4-cyano-α-methylbenzyl alcohol
F-TF	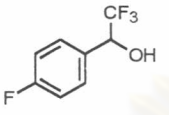	4-fluoro-α-(trifluoromethyl)benzyl alcohol
Cl-TF	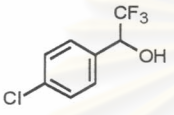	4-chloro-α-(trifluoromethyl)benzyl alcohol
Br-TF	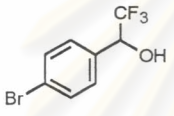	4-bromo-α-(trifluoromethyl)benzyl alcohol

4.2 Capillary Column Coating

Coated capillary columns were evaluated for their properties with Grob test mixture which composed of twelve compounds of different functional group: *n*-decane (C10); *n*-undecane (C11); methyl decanoate (E10); methyl undecanoate (E11); methyl dodecanoate (E12); nonanal (al); 1-octanol (ol); 2,3-butanediol (D); 2,6-dimethylphenol (P); 2,6-dimethylaniline (A); 2-ethylhexanoic acid (S); and dicyclohexylamine (am). Column efficiency was determined from the average separation number between E10-E11 and E11-E12 pairs. From the chromatogram, a 100% line was drawn by connecting C10, C11, E10, E11, and E12 peaks. Peaks below this line indicated some adsorption of the corresponding functional group towards the stationary phase. The acid-base property of the columns was judged from the ratio of peak height of A-P and S-am pairs.

4.2.1 OV-1701 column

Grob test chromatogram of OV-1701 column was shown in figure 4.1. This column has high efficiency with the average separation number of 42.7. This value is also in good agreement with the efficiency obtained by isothermally testing

with *n*-alkanes in the temperature range of 50-200 °C (3000-4000 plates/meter). This indicates that OV-1701 column can be used efficiently at both high and low temperatures. This column showed no adsorption towards alcohol (ol), but exhibited some adsorption towards diol (D) and aldehyde (al). Besides, it is not recommended for the analysis of underivatized carboxylic acids (S) or amines (am).

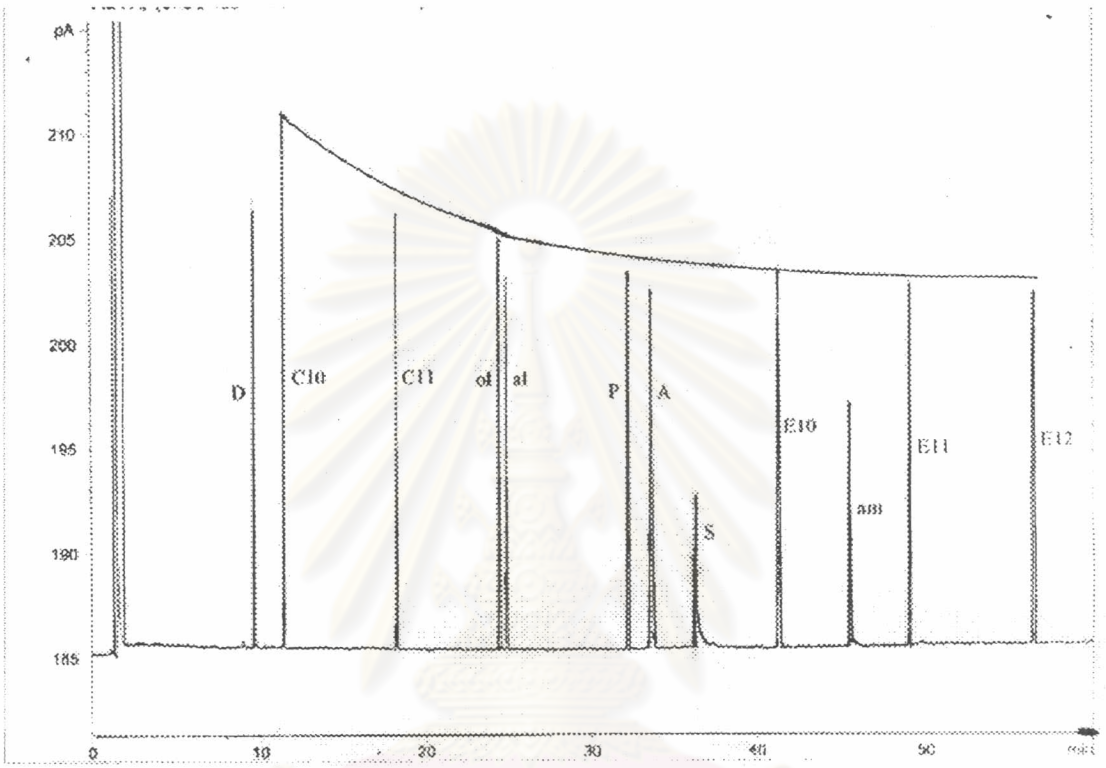

Figure 4.1 A chromatogram of the Grob test mixture on a 32.40 m long, 0.25 mm i.d. capillary, coated with 0.25 μm film of OV-1701. Temperature program: 40-160 °C at 1.54 °C/min.

4.2.2 BSiMe column

BSiMe column also exhibited high efficiency over a wide range of temperatures with the average separation number of 43.7. This stationary phase showed slight adsorption towards diol (D) and aldehyde (al), and is not suitable for the separation of underivatized carboxylic acids (S) and amines (am). Interestingly, diol (D) was observed as two peaks of isomers and the separation of chiral acid (S) could be detected, as shown in figure 4.2, due to the selectivity of the derivatized cyclodextrin.

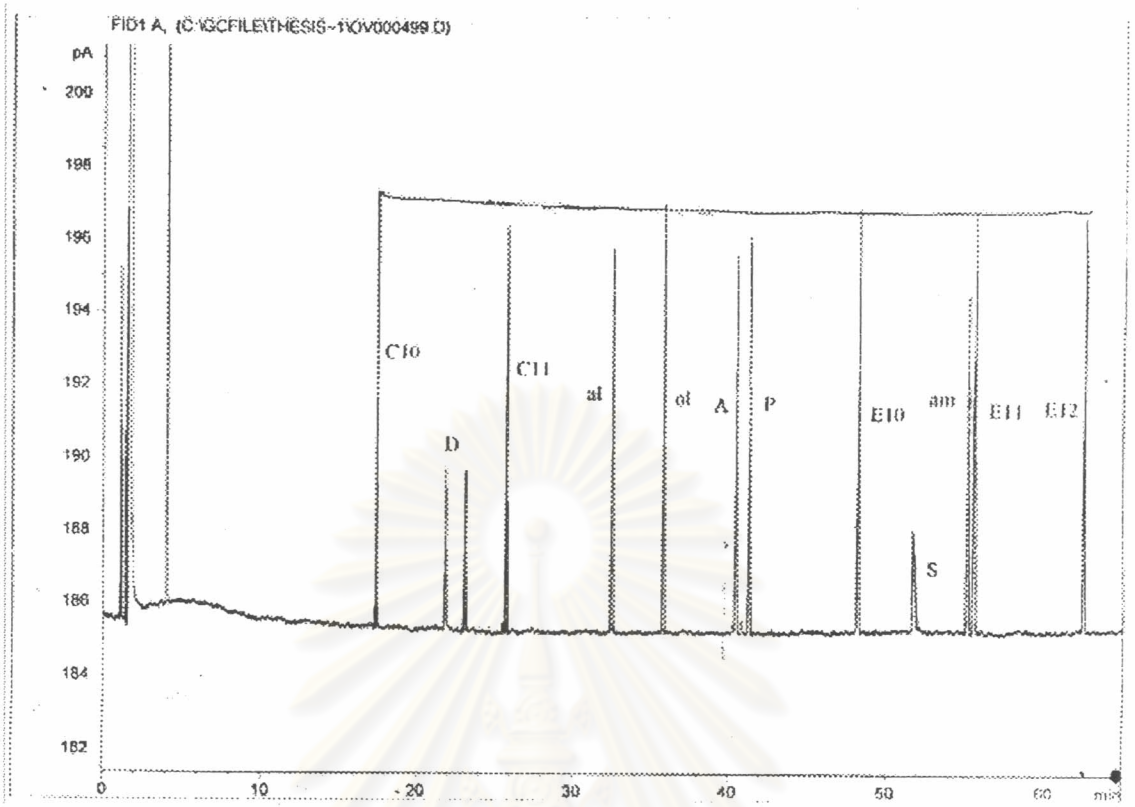

Figure 4.2 A chromatogram of the Grob test mixture on a 31.80 m long, 0.25 mm i.d. capillary, coated with 0.25 μm film of 25.5% BSiMe in OV-1701. Temperature program: 40-160 °C at 1.57 °C/min.

4.2.3 BMe column

Column performance of BMe phase could not be evaluated by Grob test as the stationary phase becomes solid at low operating temperature (below 130 °C). The column efficiency was then obtained isothermally from *n*-alkanes and was in the 2000 plates/meter range. Adsorptive characteristic of this column towards alcohols (which are analytes of interest in this study) was evaluated from asymmetric factor and found to be insignificant.

4.3 Gas Chromatographic Separation of 1-Phenylethanol Derivatives

All chiral alcohols were analyzed isothermally on three columns in the temperature range of 130-200 °C at 10 °C interval. The retention factor and enantioselectivity of racemates at 150 °C were calculated and compared as shown in figures 4.3-4.4.

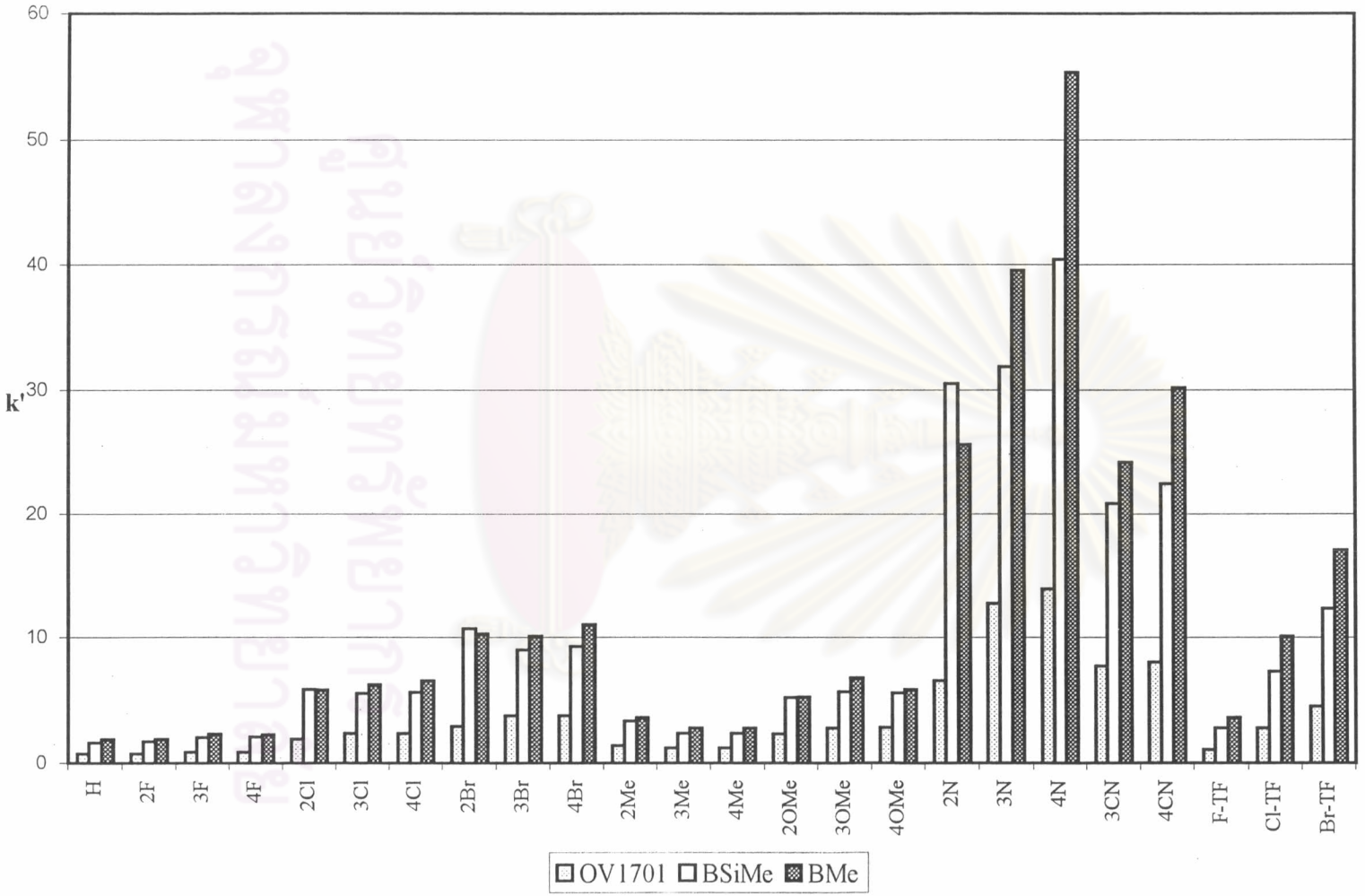

Figure 4.3 Retention factors (k′) of the more retained enantiomers of 1-phenylethanol derivatives at 150 °C on all stationary phases

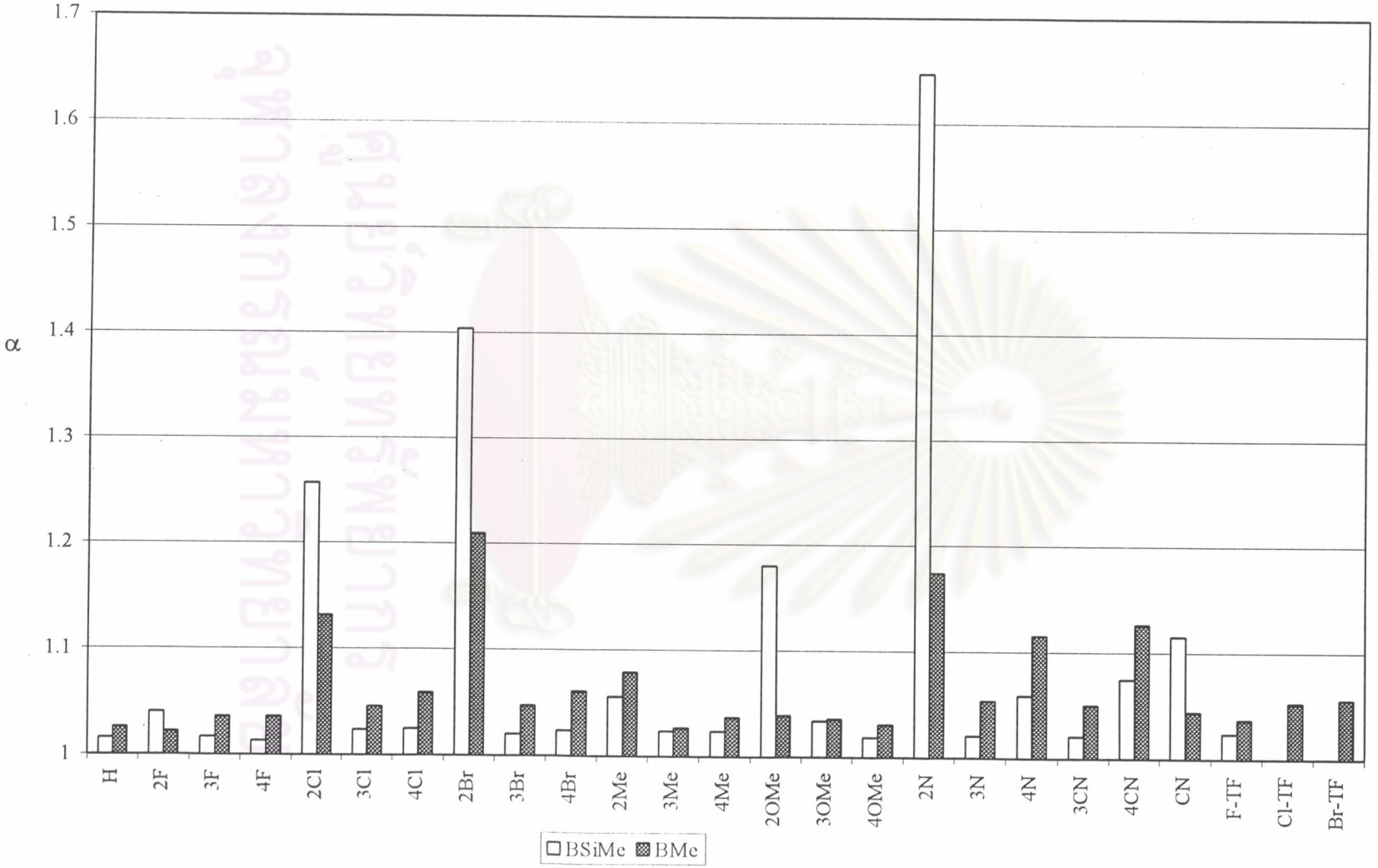

Figure 4.4 Separation factors (α) of all racemates at 150 °C on BSiMe and BMe columns

On OV-1701 column, the retention factors (k′) of all substituted 1-phenylethanol were greater than that of the unsubstituted one. As expected, the k′ values increased with the molecular weight and polarity of substituent. Compounds with the same substituent, regardless of position, exhibited similar retention (e.g. **2F**, **3F**, and **4F** have the k′ of 0.76, 0.89, and 0.86, respectively). Nitro-substituted 1-phenylethanols were the only exception, where the retention of **2N** was much smaller than those of **3N** and **4N** (k′ of 6.56 for **2N** compared to 12.76 and 13.94 for **3N** and **4N**, respectively). Compounds with the same substituent type displayed an increase in retention as the molecular weight increased. For instance, the retention of halogen-substituted derivatives increased as the atomic weight of the substituent increased in the order of fluoro, chloro, to bromo. Another example was observed in the electron-withdrawing series, the retention of nitro-substituted alcohols was greater than that of cyano-substituted ones.

The retention of all analytes on two CD-containing columns, BSiMe and BMe, was larger than that on OV-1701 column. This suggested that CD derivatives were responsible for an increase in retention in view of the fact that all three columns contain polysiloxane as a major component and have identical film thickness. It was observed that the retention of most analytes obtained from BMe column is slightly higher than from BSiMe column. This is probably due to the higher interaction of polar analytes toward higher polarity CD derivative, BMe. However, the tendency of retention in each chiral column was very similar to that of OV-1701 column.

The selectivity factor, on the other hand, exhibited different trend from the retention. It was noticed that all racemic alcohols studied could be resolved into their corresponding enantiomers on BMe column. In general, the separation was improved as the substituent size became larger. Nonetheless, the position of the substituent seemed to have a stronger effect on the selectivity than the size does on both columns. Analytes with substituent at the *ortho* position showed better separation than those at the *meta* and *para* positions (figure 4.5). Comparing the selectivity of both columns, it was observed that the selectivity of BMe derivative toward *meta*- and *para*-substituted 1-phenylethanol is slightly higher than that of BSiMe. However, the selectivity of BSiMe toward *ortho*-substituted derivatives is superior than that of

BMe, particularly for the derivatives with large substituents such as nitro, bromo, and chloro (figure 4.6).

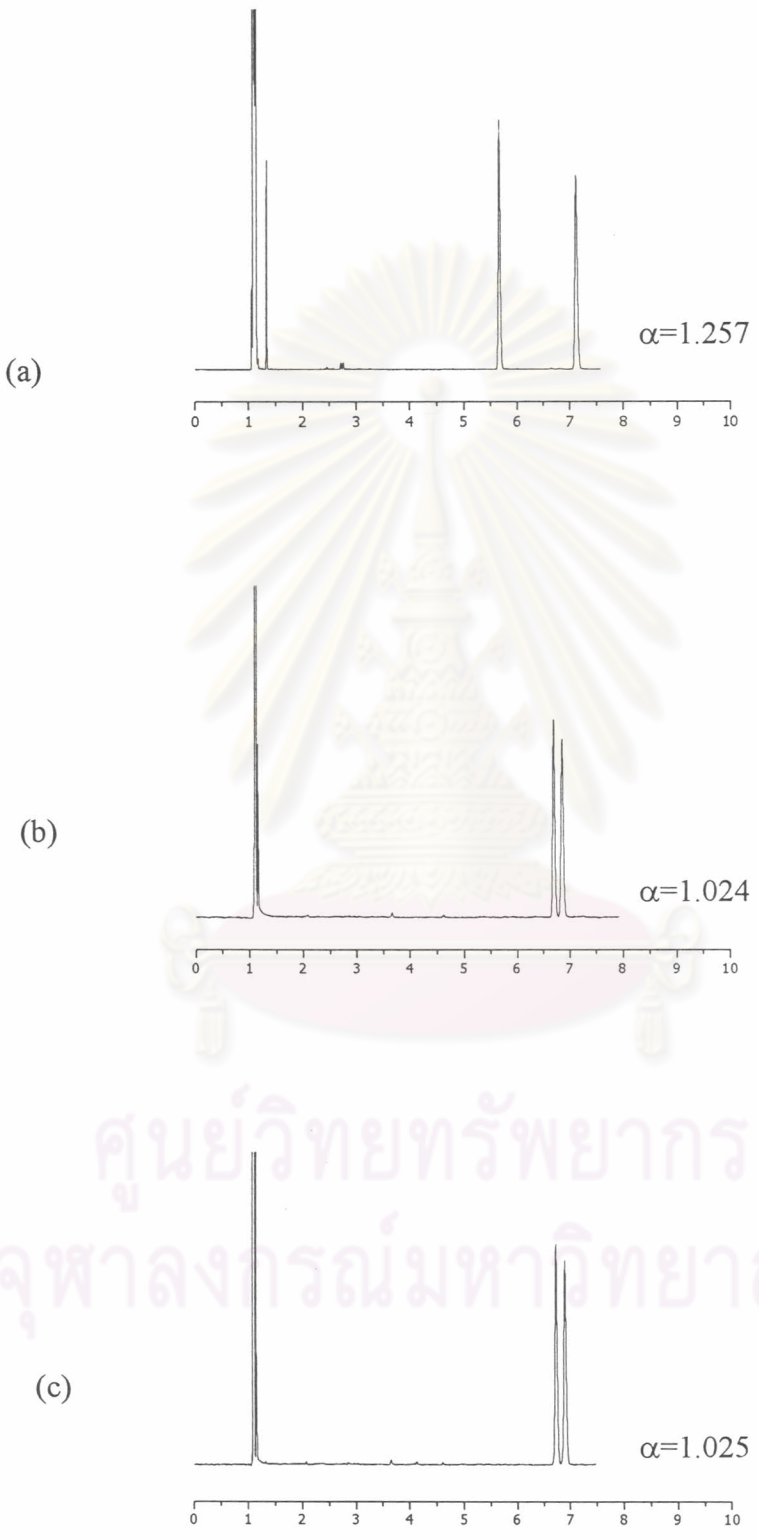

Figure 4.5 Chromatograms of (a) **2Cl**; (b) **3Cl**; and (c) **4Cl** at 150 °C on BSiMe column

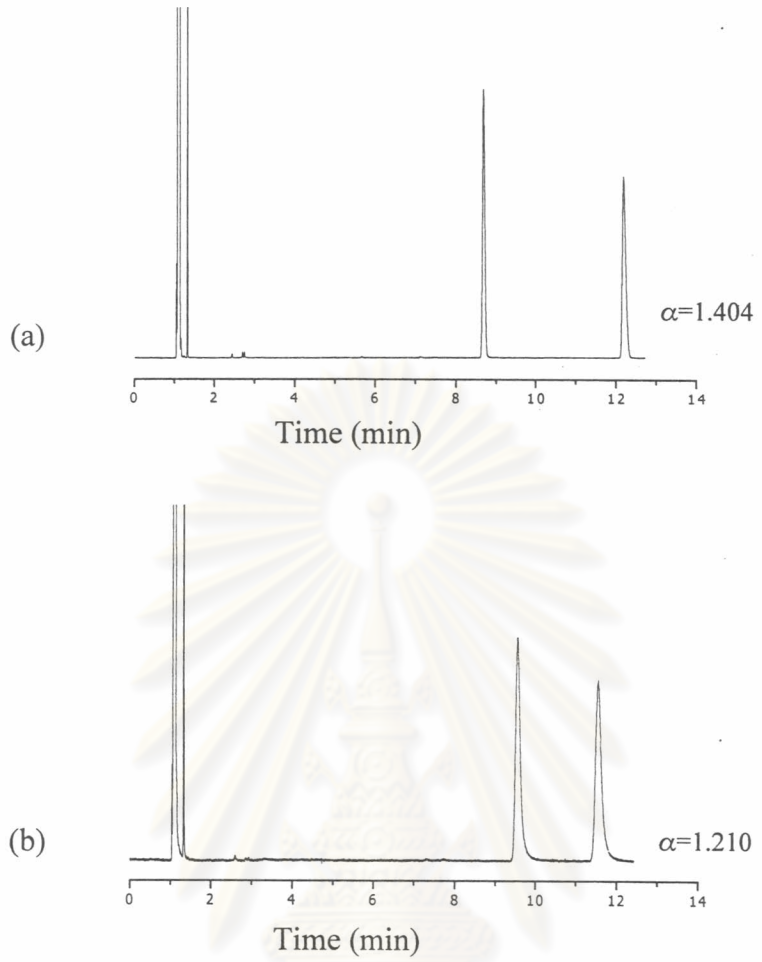

Figure 4.6 Chromatograms of **2Br** at 150 °C on (a) BSiMe and (b) BMe columns

Since the retention and selectivity factors of analytes at a particular temperature could not reveal the nature of interaction between analytes and cyclodextrin derivatives, thus thermodynamic parameters (e.g. enthalpy and entropy) responsible for the formation of diastereomeric complexes needed to be determined.

4.4 Thermodynamic Parameters

4.4.1 Method A

Enthalpy (-ΔH) and entropy (-ΔS) values of each enantiomer could be determined from the relationship between ln k′ and reciprocal of absolute temperature, according to equation (5). All plots are linear with correlation coefficient mostly greater than 0.997. The enthalpy and entropy values of the more retained enantiomers on two chiral columns, compared to the values on nonchiral column, were depicted in figures 4.7-4.8, respectively.

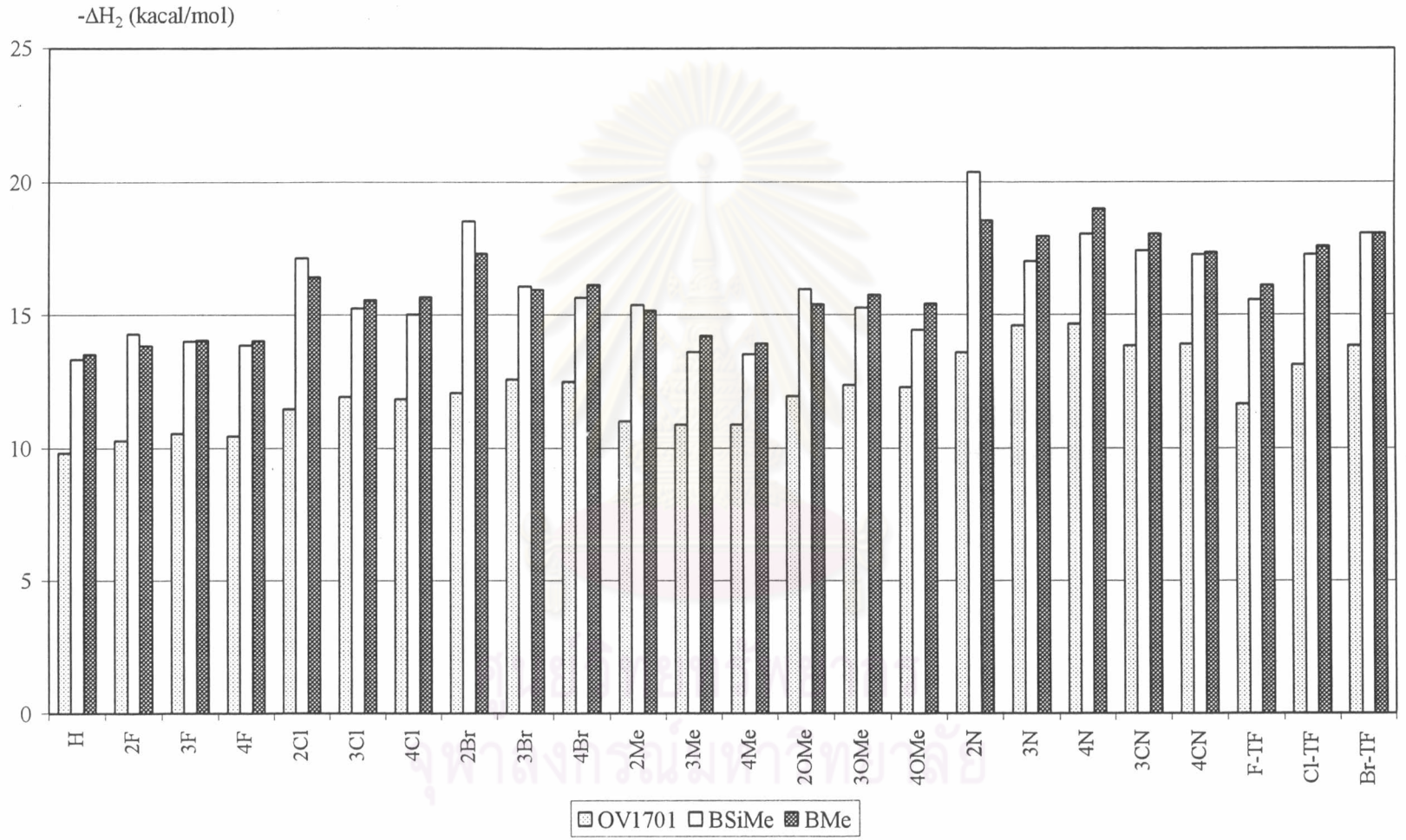

Figure 4.7 Enthalpy values of the more retained enantiomers on all three columns calculated by method A

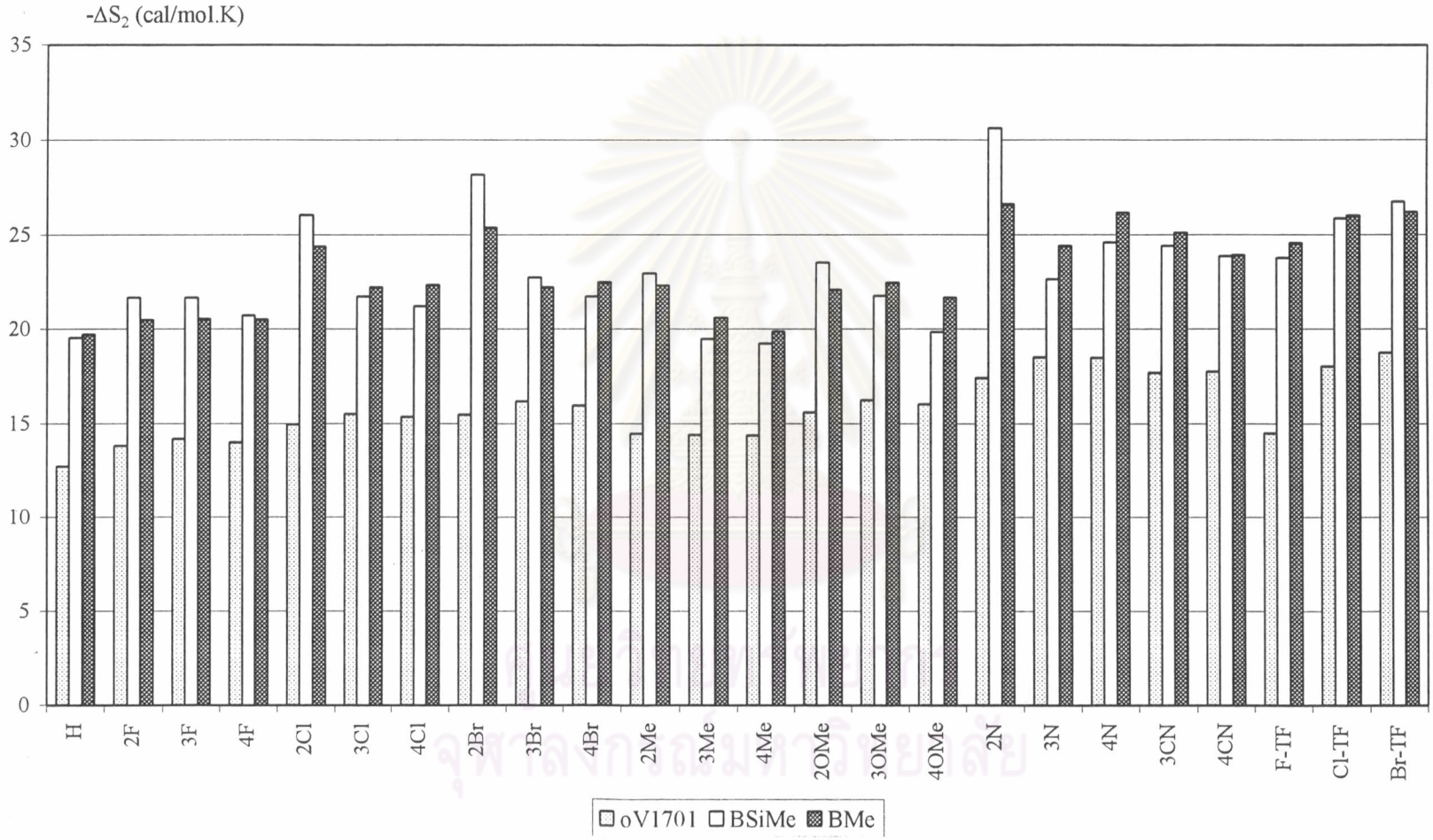

Figure 4.8 Entropy values of the more retained enantiomers on all three columns calculated by method A

The enthalpy value (-ΔH), in figure 4.7, represented the strength of interaction between an analyte and stationary phase: the higher the value (more negative value), the higher the strength of interaction. The negative entropy value, on the other hand, denoted the loss of degree of freedom resulted from the interaction between the enantiomer and stationary phase. Both enthalpy and entropy values on a medium-polarity OV-1701 column displayed a similar trend as the retention factors, i.e. the strength and the loss of degree of freedom increase as the molecular weight and polarity of analyte increase.

On BSiMe column, it can be seen that -ΔH and -ΔS values of most analytes are similar to each other and closed to the value of 1-phenylethanol, except for the large substituents at the *ortho* position (**Cl**, **Br**, **N**) and cyano substituent where the larger values were observed. The thermodynamic values on BMe column, on the other hand, did not show a noticeable trend as in the BSiMe column. This observation indicates that the major contribution to the strength of interaction and the degree of freedom would probably come from the hydroxy group of 1-phenylethanol derivatives since thermodynamic parameters of all analytes were quite similar.

Thermodynamic parameters corresponding to the separation of enantiomers of 1-phenylethanol and it derivatives could be determined either from the difference in enthalpy and entropy values or from the plot of ln α vs.1/T. In this study, the first approach was selected. The -Δ(ΔH) and -Δ(ΔS) values of 1-phenylethanol and derivatives are depicted in figures 4.9-4.10.

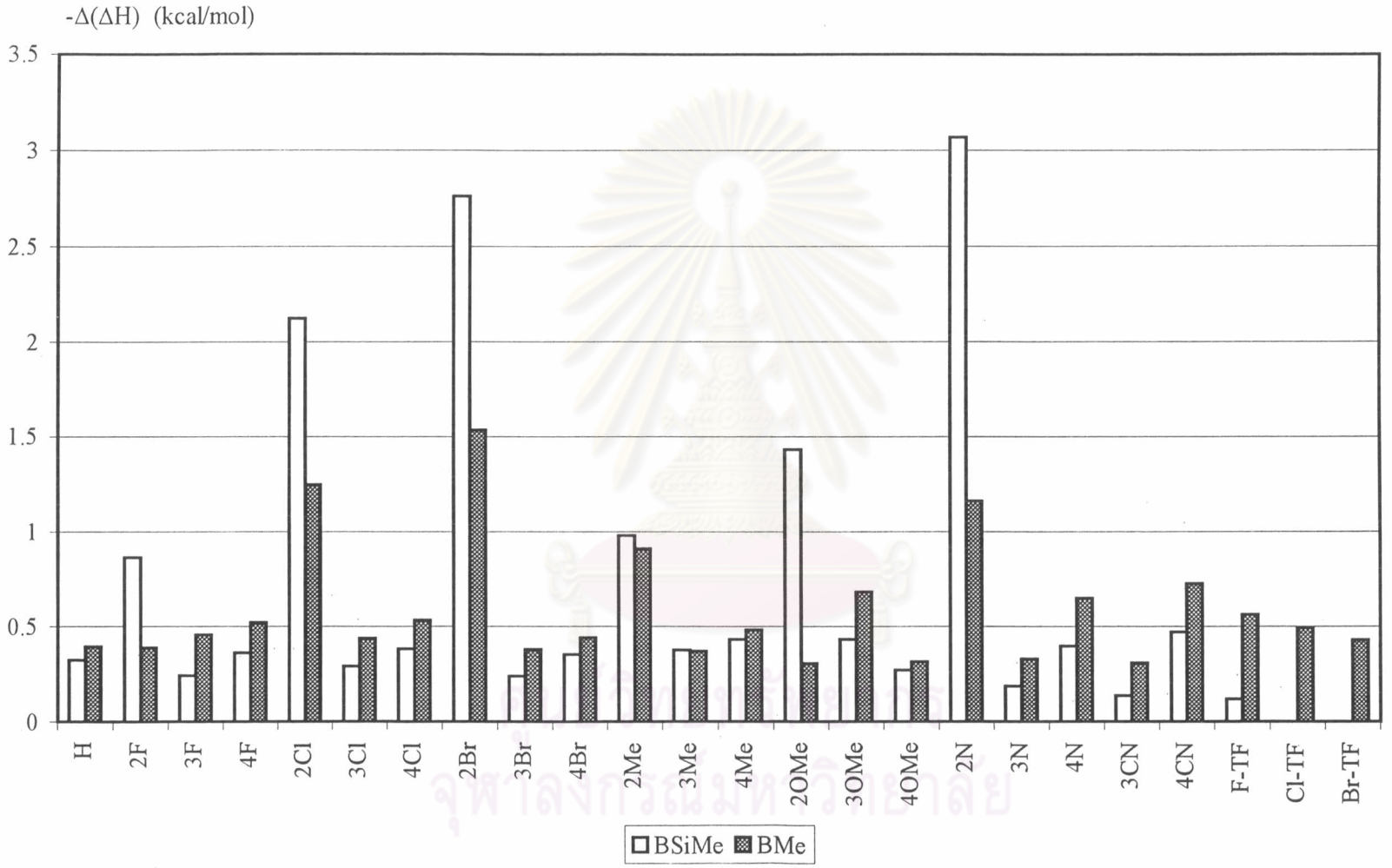

Figure 4.9 Differences in enthalpy values of enantiomers on BSiMe and BMe columns calculated by method A

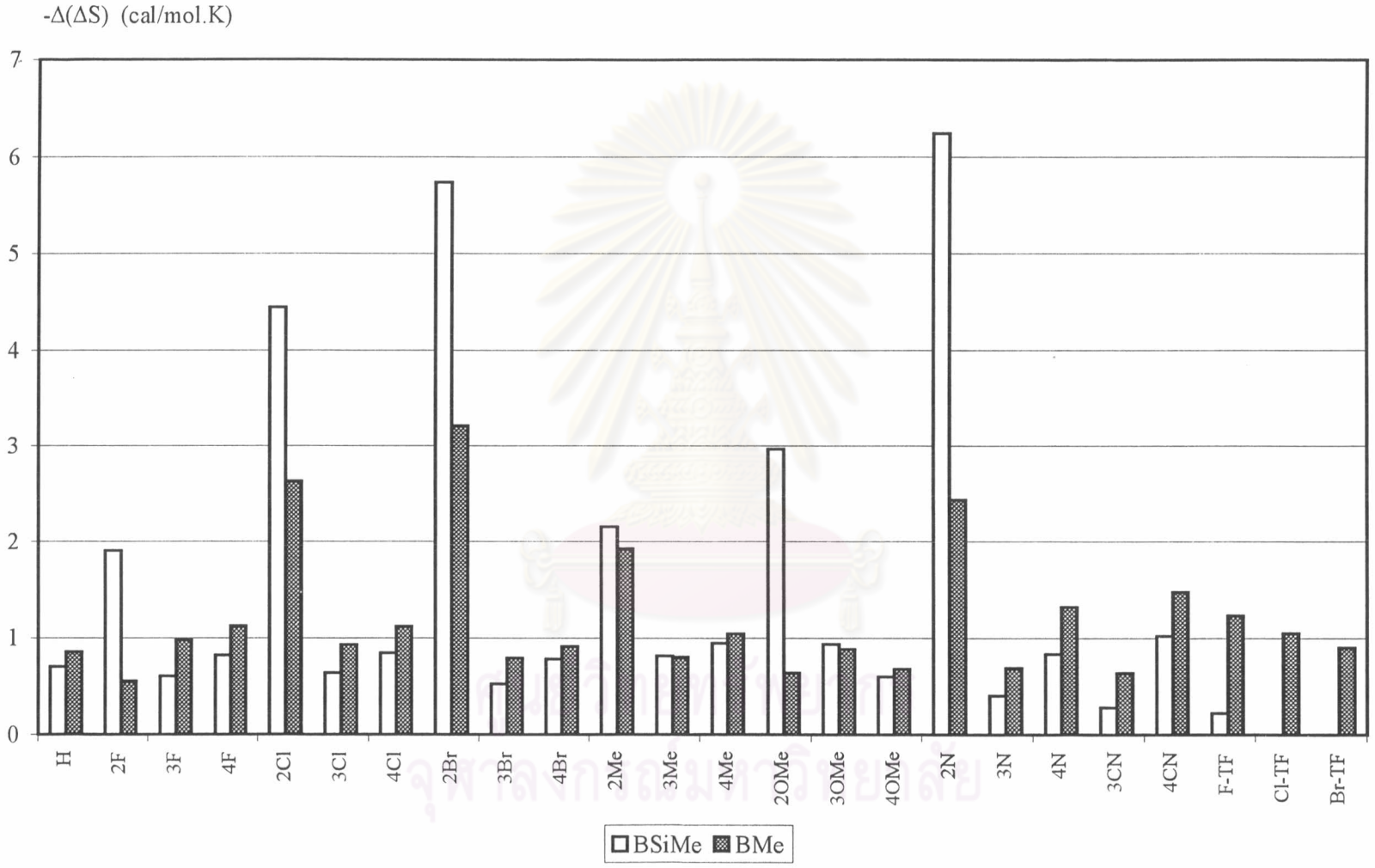

Figure 4.10 Differences in entropy values of enantiomers on BSiMe and BMe columns calculated by method A

Considering the separation of 1-phenylethanol (**H**) on both chiral columns, it was found that enantioselectivities of two CD derivatives towards **H** are very similar and was in good agreement to that investigated by Kobor et al. [25]. This can be described to the strong intermolecular interaction between polar alcohol and CD as well as polar siloxane matrix. Kobor et al. also proposed that the enantioselectivity for polar solutes, such as **H**, should be less dependent on the van der Waals interaction or the flexibility of CD selector. However, the size, shape, and flexibility of the CD selector become significant when a substituent of various size and polarity is introduced into different part of the analyte molecule.

It can be seen that, on both columns, the position of substituent played a major role to enantioselectivity than the type of substituent since the $-\Delta(\Delta H)$ and $-\Delta(\Delta S)$ values of all analytes are very similar, except the values of *ortho*-substituted analytes. Additionally, the selectivities of *ortho*-substituted analytes containing the same type of substituent increase as the molecular weight increases. As seen in figures 4.11-4.12, the separation of **2F** on BSiMe is greater than that of **3F**, **4F**, or unsubstituted alcohol (**H**) and the selectivity increases from **2F** to **2Cl** to **2Br**.

Even though *ortho*-substituted analytes could be clearly resolved on both columns, the BSiMe provided higher selectivity towards this type of analytes than BMe did (figure 4.13). In contrast to the characteristic of BSiMe towards *ortho*-substituted alcohols, BMe offered slightly better separation towards *meta*- and *para*-substituted alcohols than BSiMe. Considering the structure of BSiMe and BMe, both CD derivatives possess the same *O*-methyl substituents at the C2 and C3 chiral carbons. However, the substituents at the C6 nonchiral carbons located at the narrow opening of the cavity are different. The large and bulky *O*-*tert*-butyldimethylsilyl groups of BSiMe, instead of the small *O*-methyl groups of BMe, at C6 of glucose units possibly create a more rigid and narrower cavity [25]. The less flexible geometry of BSiMe probably makes the formation of temporary diastereomeric complex between one enantiomer and CD much more favorable and, thus, result in a better enantioselectivity as shown in figure 4.13.

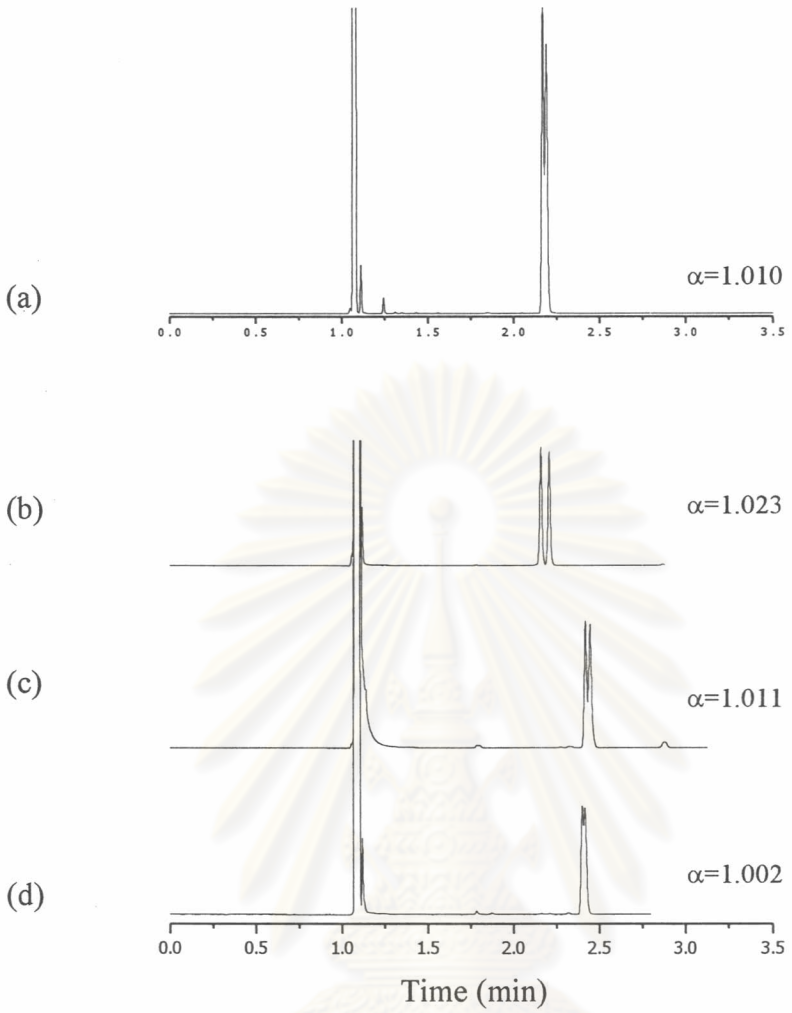

Figure 4.11 Chromatograms of (a) **H**; (b) **2F**; (c) **3F**; and (d) **4F** at 160 °C on BSiMe column

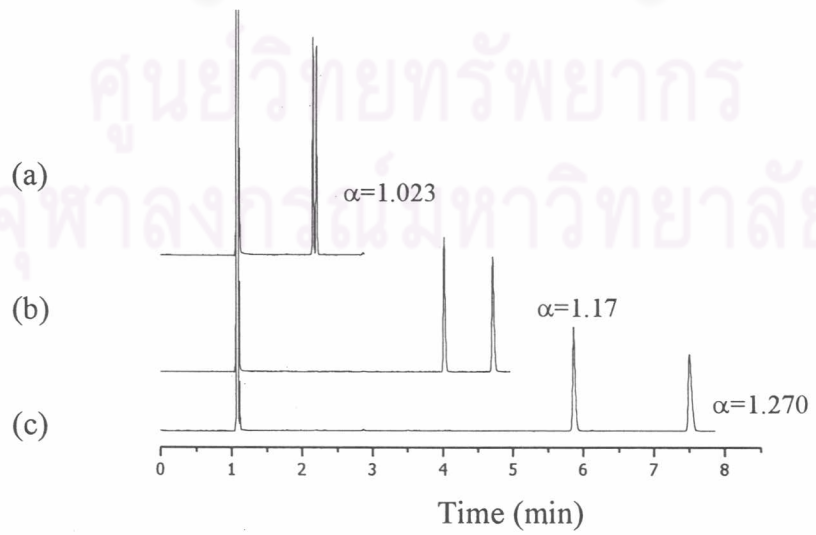

Figure 4.12 Chromatograms of (a) **2F**; (b) **2Cl**; and (c) **2Br** at 160 °C on BSiMe column

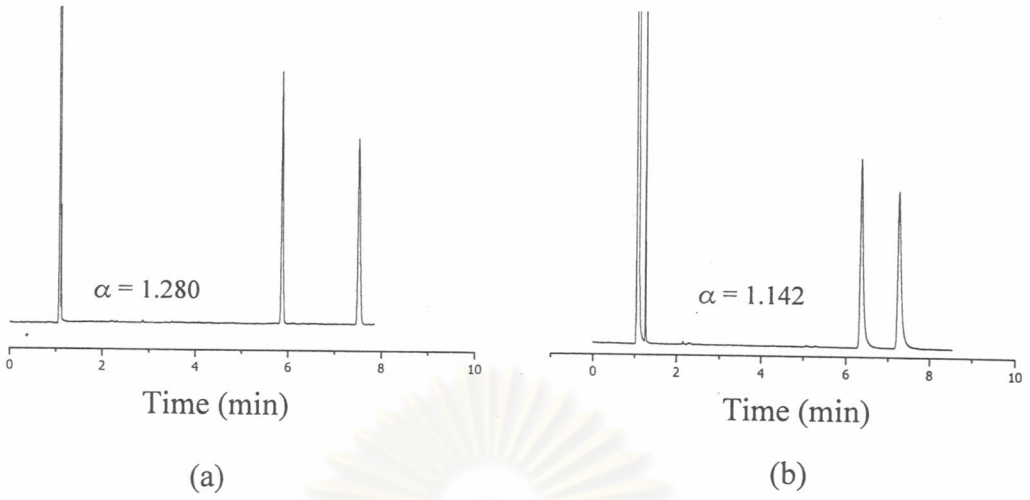

Figure 4.13 Chromatograms of **2Br** at 160 °C on (a) BSiMe and (b) BMe columns

Three α-(trifluoromethyl) derivatives of benzyl alcohol (**F-TF**, **Cl-TF**, **Br-TF**) were also prepared to explore the effect of α-(trifluoromethyl) substituent on enantioselectivity. Since BSiMe showed comparable chiral selectivity (-Δ(ΔH) and -Δ(ΔS) values) for **H**, **4F**, **4Cl**, and **4Br**, it was expected to observe similar selectivity for **F-TF**, **Cl-TF**, and **Br-TF**. Despite the equal size of hydrogen and fluorine atoms, the polarizability of trifluoromethyl group at the chiral center of the analyte molecules considerably influence the separation on BSiMe column. The difference in enthalpy and entropy values of α-(trifluoromethyl) derivatives of benzyl alcohol decreased drastically and only separation of **F-TF** was observed. Surprisingly, the α-(trifluoromethyl) substituent has no impact on the separation on BMe column (figure 4.14). This is a clear evidence that the substituent at the nonchiral carbons of CD molecule can bring about the change in CD shape and; consequently, result in a change in enantioselectivity.

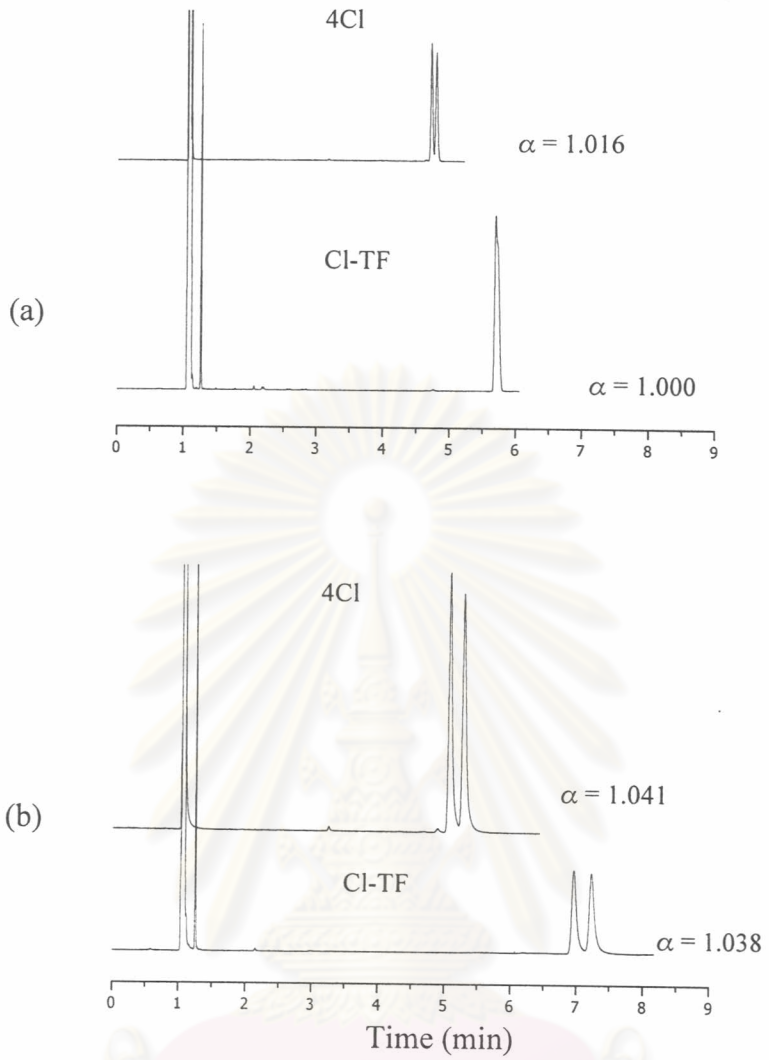

Figure 4.14 Chromatograms of **4Cl** and **Cl-TF** at 160 °C on (a) BSiMe and (b) BMe columns

4.4.2 Method B

Enthalpy (-ΔH) and entropy (-ΔS) values responsible for the interaction between each individual enantiomer and CD derivative could be determined from the relationship between ln R′ and reciprocal of absolute temperature, according to equation (10). All relationships were linear with correlation coefficient mostly greater than 0.97. The differences in thermodynamic values of enantiomeric pairs accountable for the separation were then calculated. The enthalpy and entropy values of the more retained enantiomers obtained from two chiral columns were shown in figures 4.15 -4.16, respectively. The enthalpy and entropy

differences (-Δ(ΔH) and -Δ(ΔS) values) were also depicted in figures 4.17-4.18, respectively.

As illustrated in figures 4.15-4.18, the *ortho*-substituted alcohols still exhibited stronger interaction (high -ΔH and -ΔS) than analytes with substituent at *meta* or *para* position. Nonetheless, the size, molecular weight, or polarity of substituent do not substantially affect the interaction, especially on BMe column, since the -ΔH and -ΔS values did not show a significant increase as those aforementioned parameters changed. As a result, an increase in the interaction as the size, molecular weight, or polarity increased should come from polysiloxane solvent. As the thermodynamic values obtained by two different methods for each chiral column were compared in figures 4.19-4.22, it can be seen that the major contribution to retention on BMe column was from nonchiral part, OV-1701.

Enthalpy and entropy values calculated by method B are normally lower than those obtained by method A. The reason is that the values obtained by method A include all interactions both from CD derivative and from polysiloxane matrix while those obtained by method B are contribution only from modified CD. The unexpected higher entropy values observed on BSiMe column for **H**, **2OMe**, and **3N** (figure 4.20) were probably caused by the non-ideal behavior of *n*-alkanes used in this study or the contribution from CD and polysiloxane was not a direct addition.

Although there are differences in -Δ(ΔH) and -Δ(ΔS) values calculated by both methods, the trend for these values on both columns is quite similar (figures 4.23-4.26). For most compounds, the values obtained by method B are higher than those by method A. It is interesting to note that, only on BSiMe column, the values of some analytes with substitution at *ortho*-position obtained by method A are either similar or slightly higher than values obtained by method B (figures 4.23-4.24). Theoretically, the -Δ(ΔH) and -Δ(ΔS) values attained from both methods should be identical. The discrepancies are perhaps due to the normal alkanes, reference compounds used in method B, did not behave as truly inert compounds.

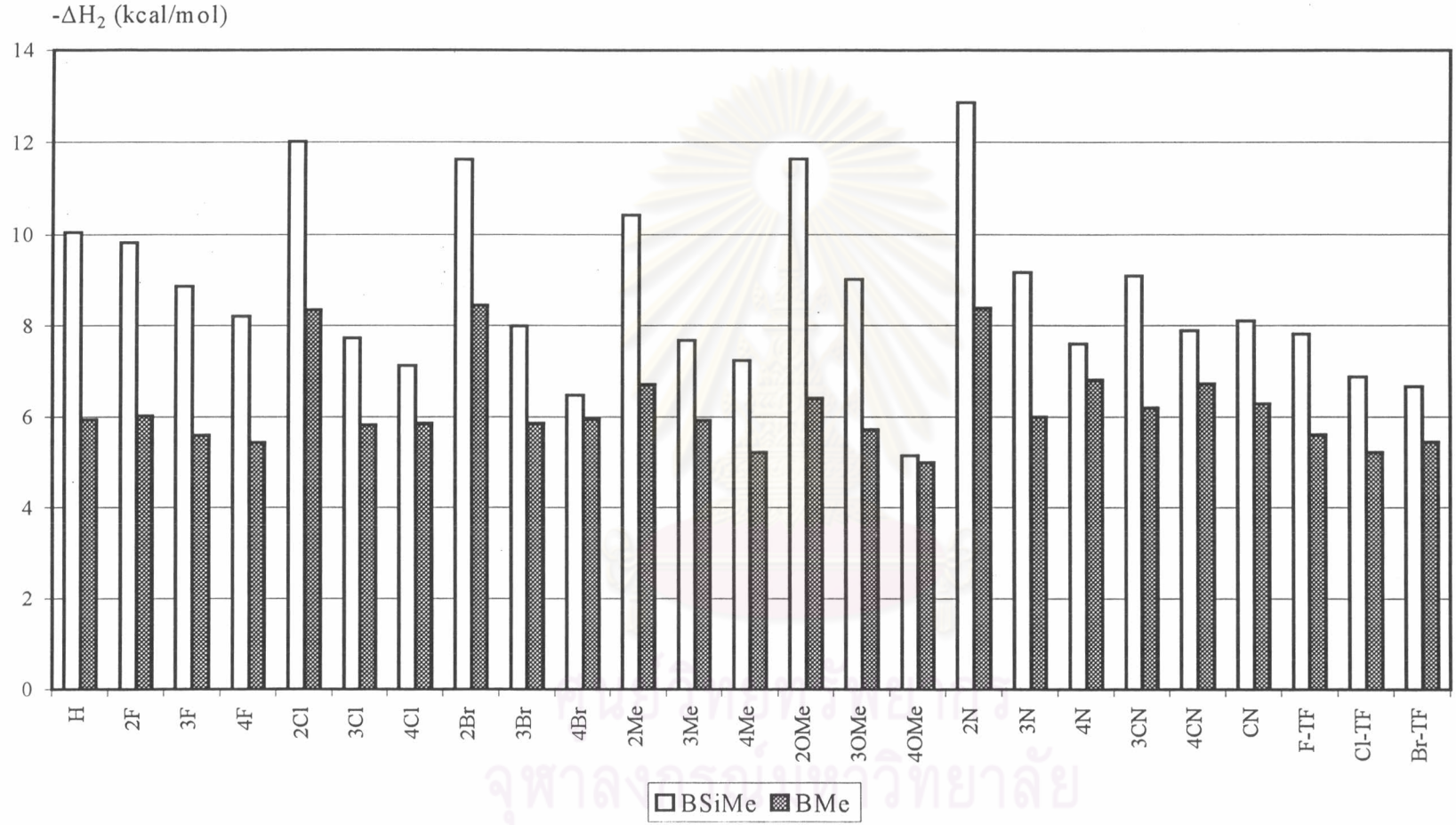

Figure 4.15 Enthalpy values of the more retained enantiomers on BSiMe and BMe columns calculated by method B

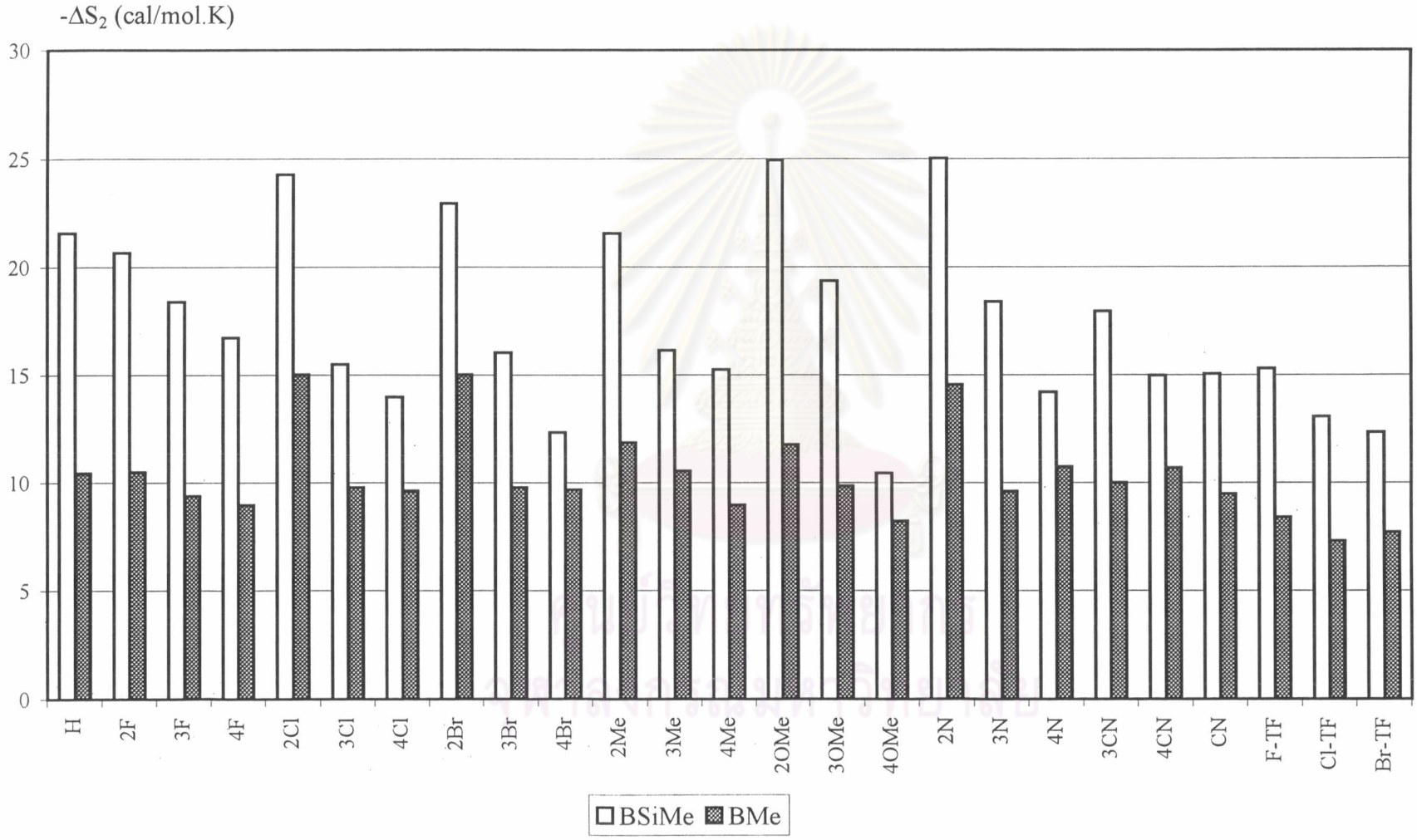

Figure 4.16 Entropy values of the more retained enantiomers on BSiMe and BMe columns calculated by method B

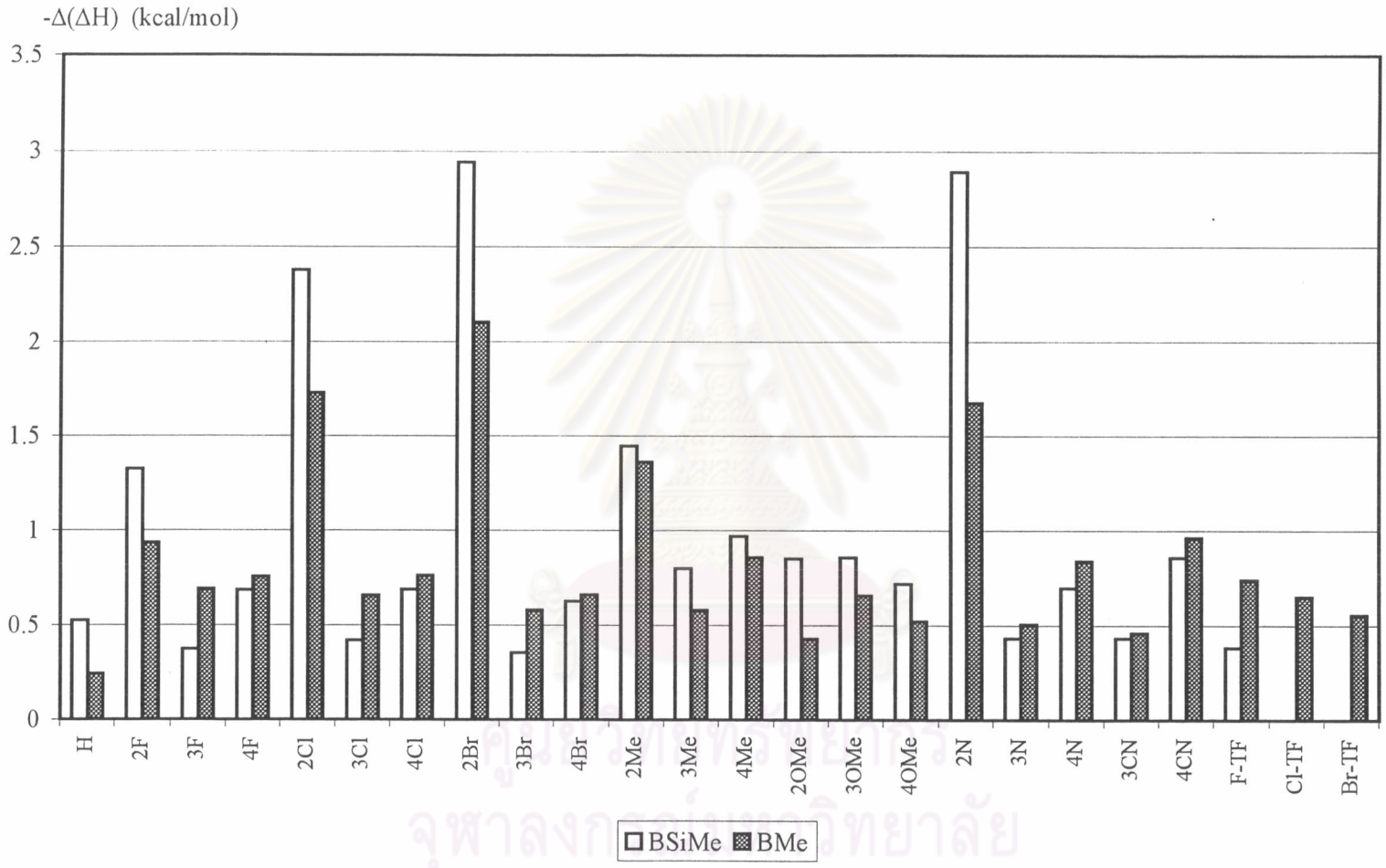

Figure 4.17 Differences in enthalpy values of enantiomers on BSiMe and BMe columns calculated by method B

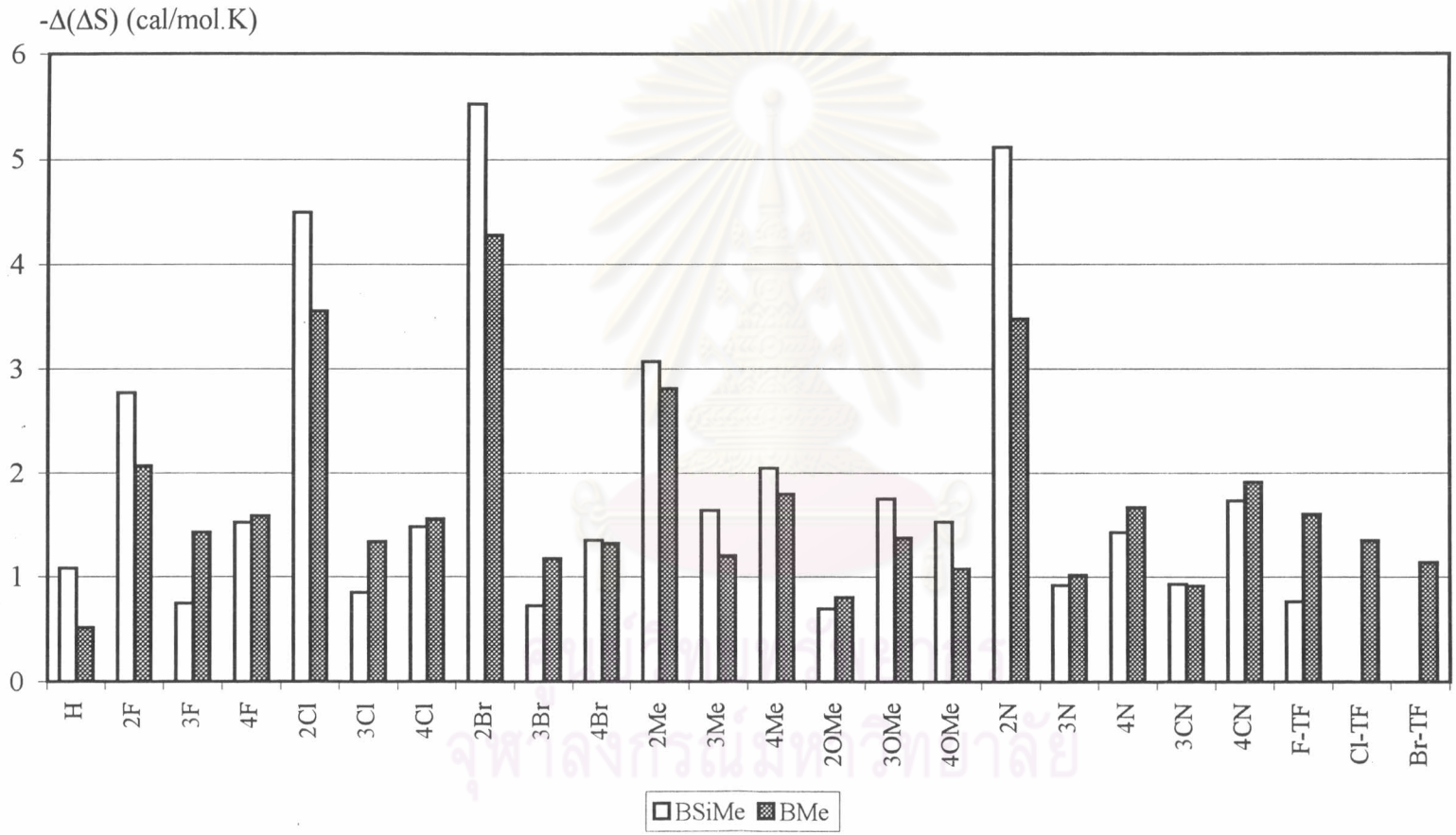

Figure 4.18 Differences in entropy values of enantiomers on BSiMe and BMe columns calculated by method B

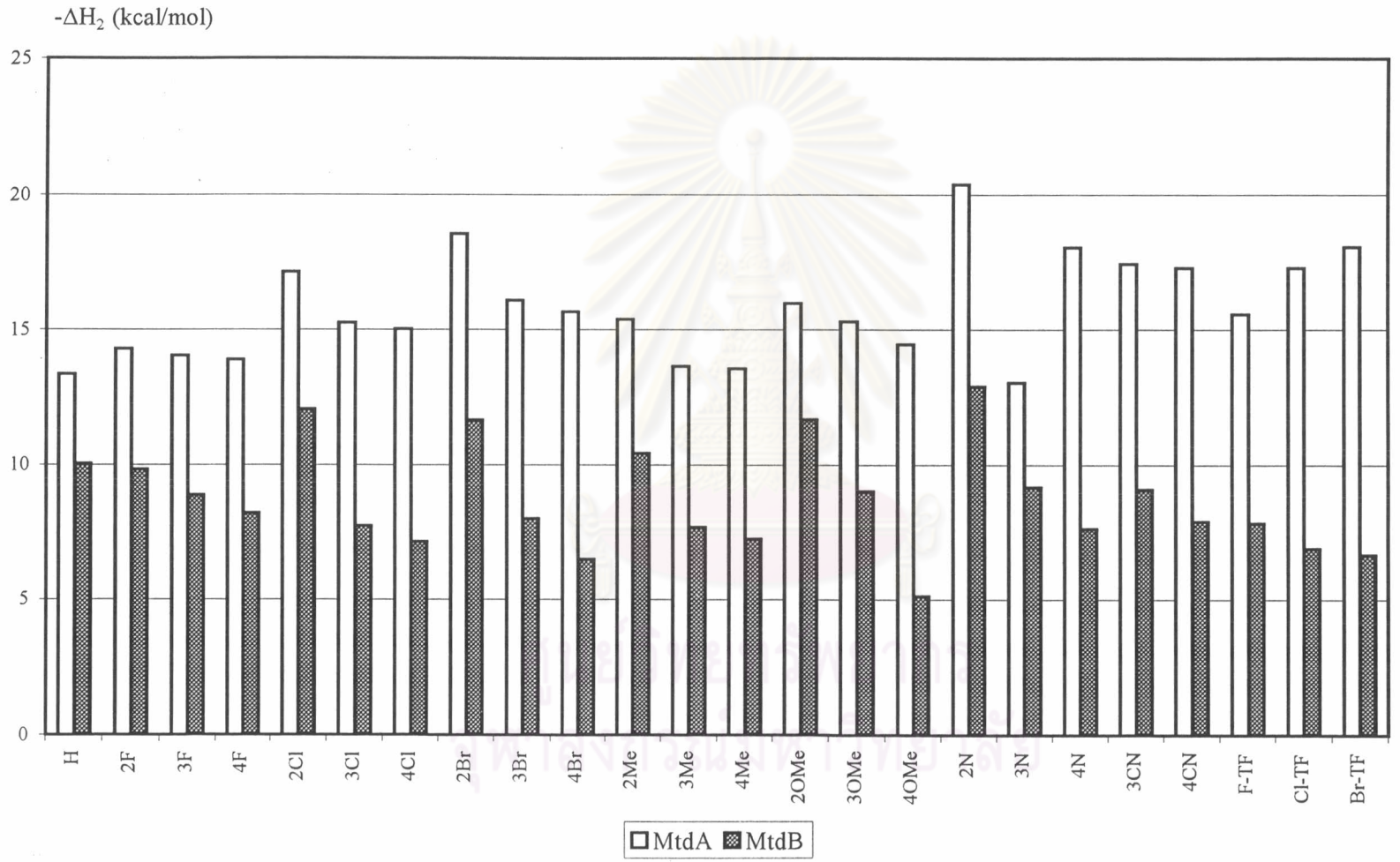

Figure 4.19 Comparison of enthalpy values of the more retained enantiomers on BSiMe column calculated by two methods

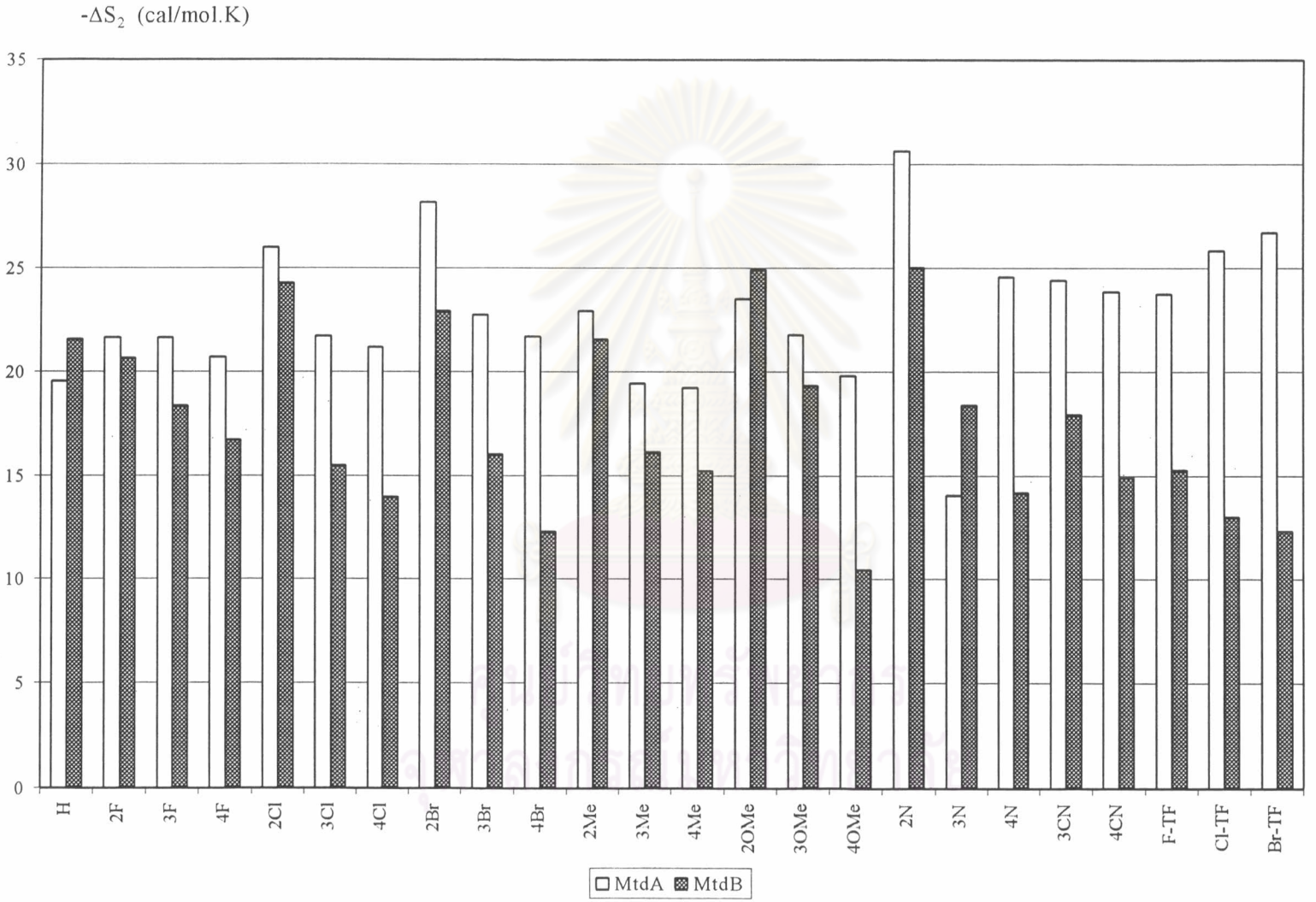

Figure 4.20 Comparison of entropy values of the more retained enantiomers on BSiMe column calculated by two methods

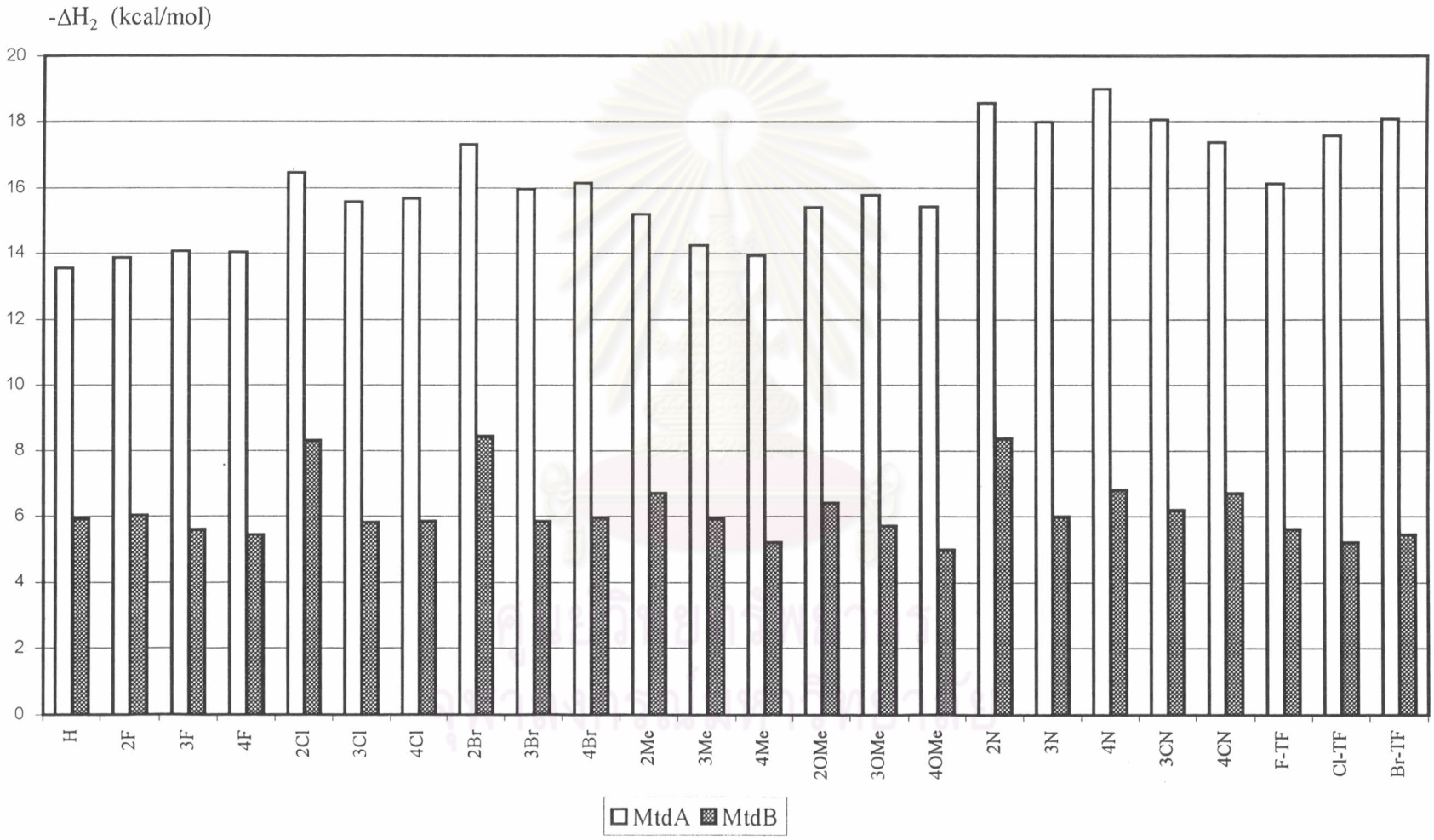

Figure 4.21 Comparison of enthalpy values of the more retained enantiomers on BMe column calculated by two methods

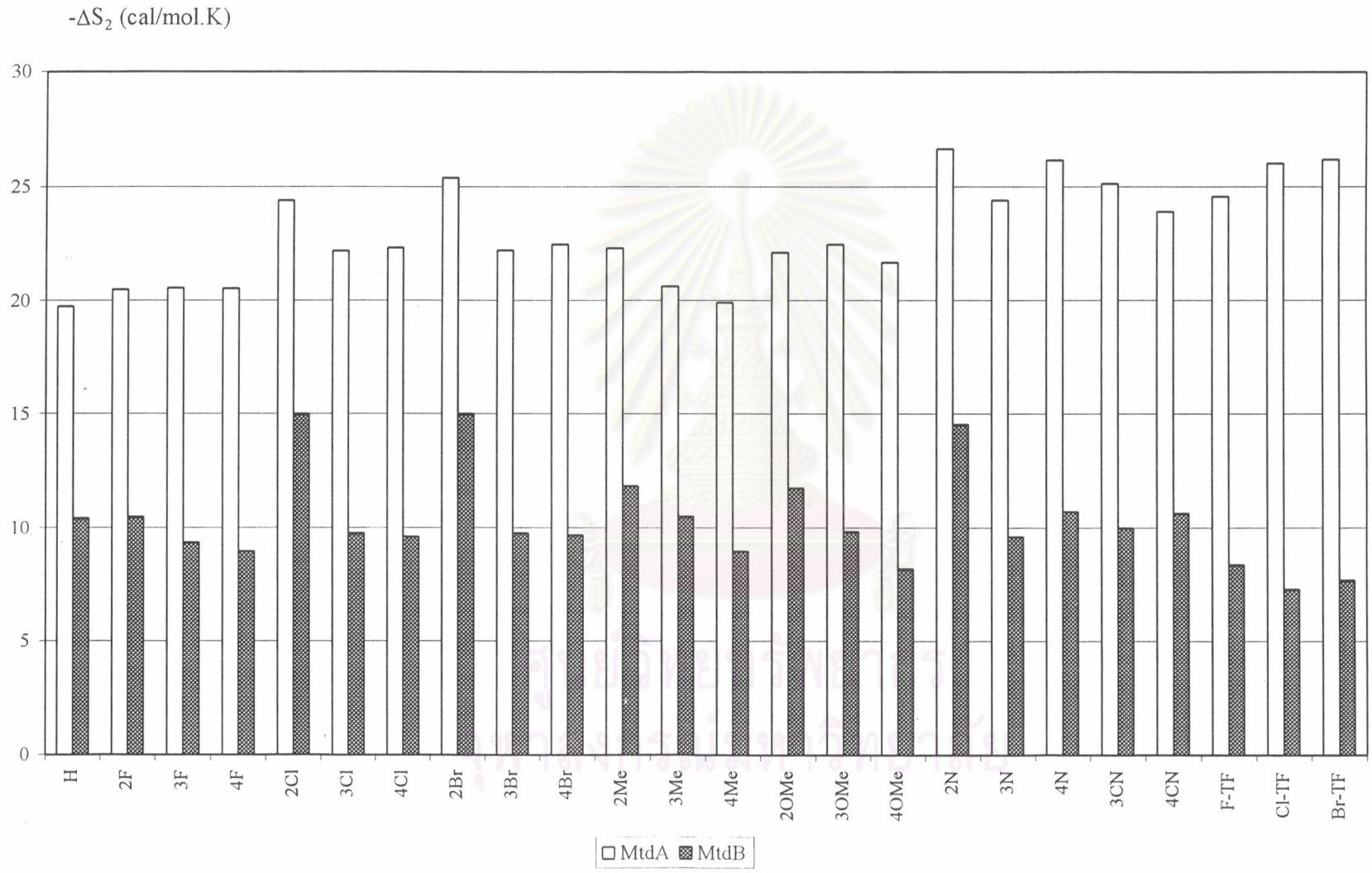

Figure 4.22 Comparison of entropy values of the more retained enantiomers on BMe column calculated by two methods

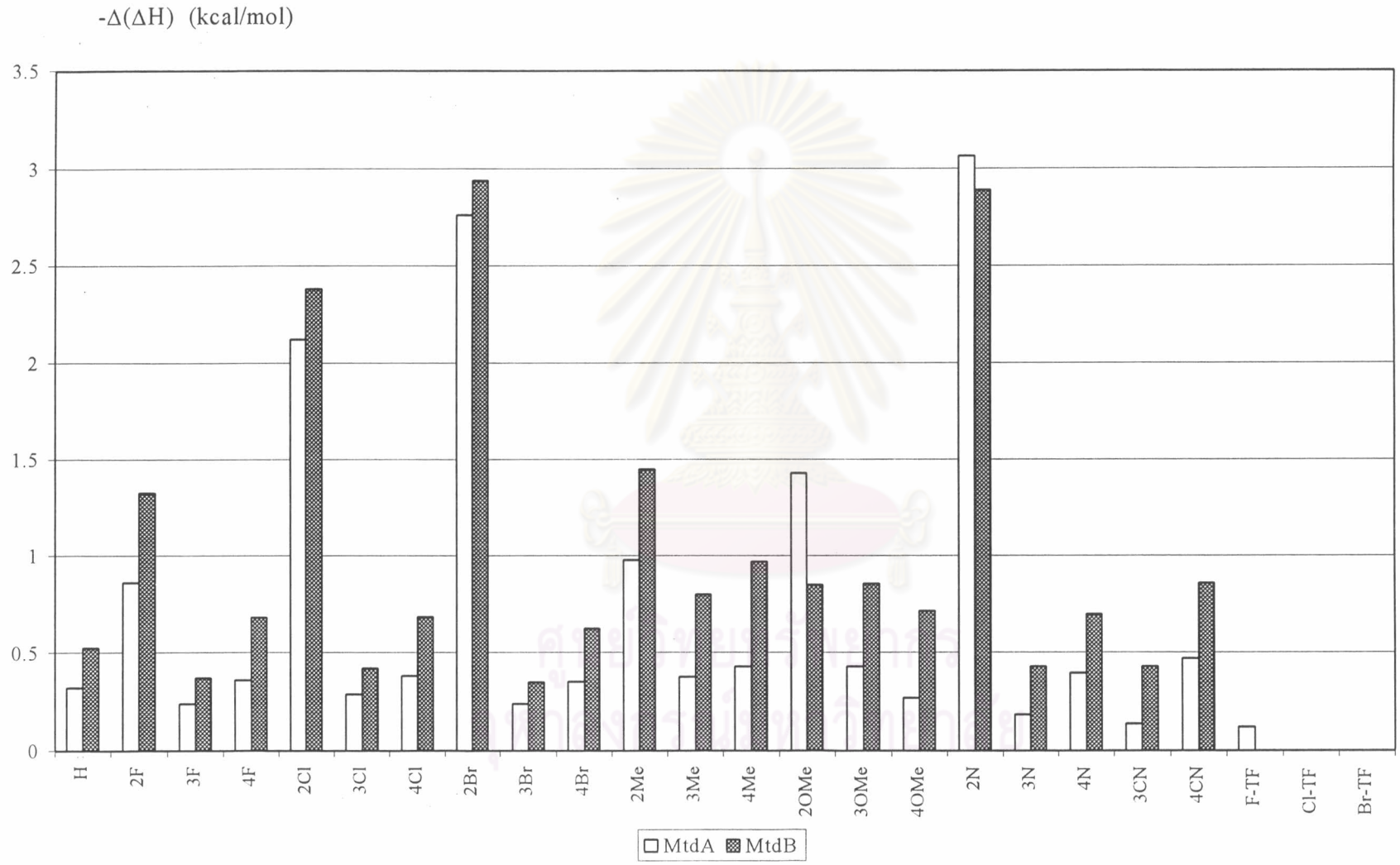

Figure 4.23 Comparison of enthalpy differences on BSiMe column calculated by two methods

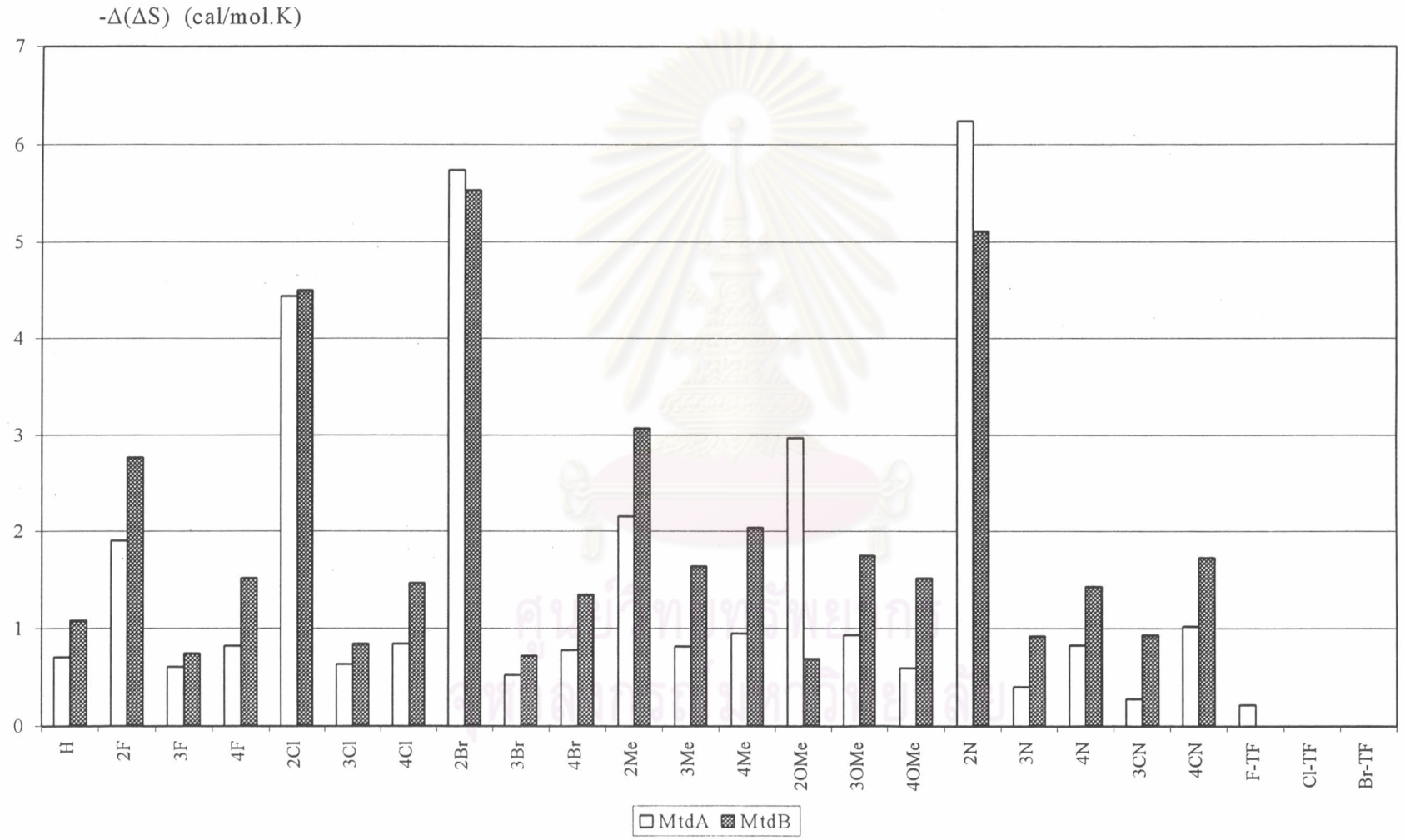

Figure 4.24 Comparison of entropy differences on BSiMe column calculated by two methods

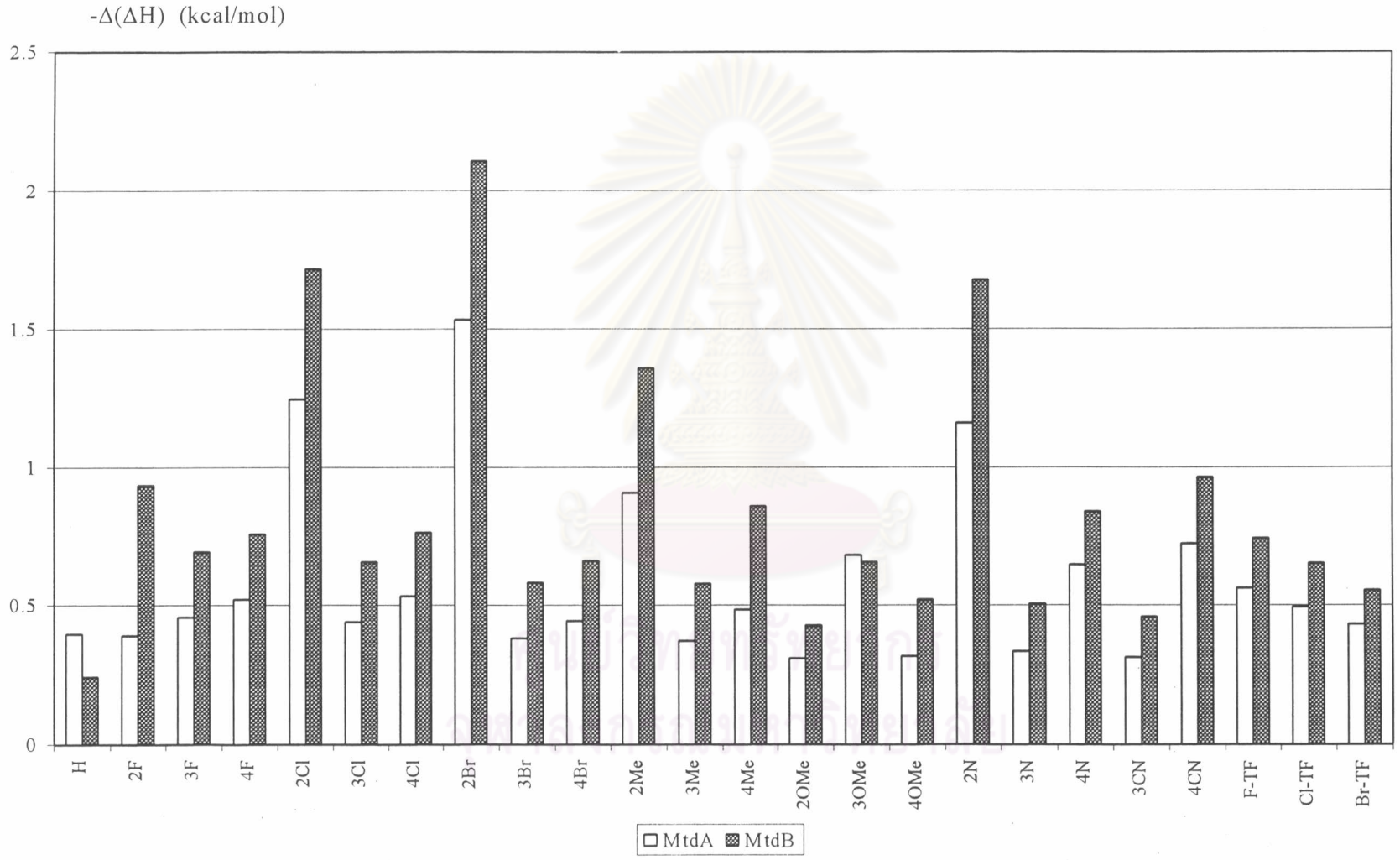

Figure 4.25 Comparison of enthalpy differences on BMe column calculated by two methods

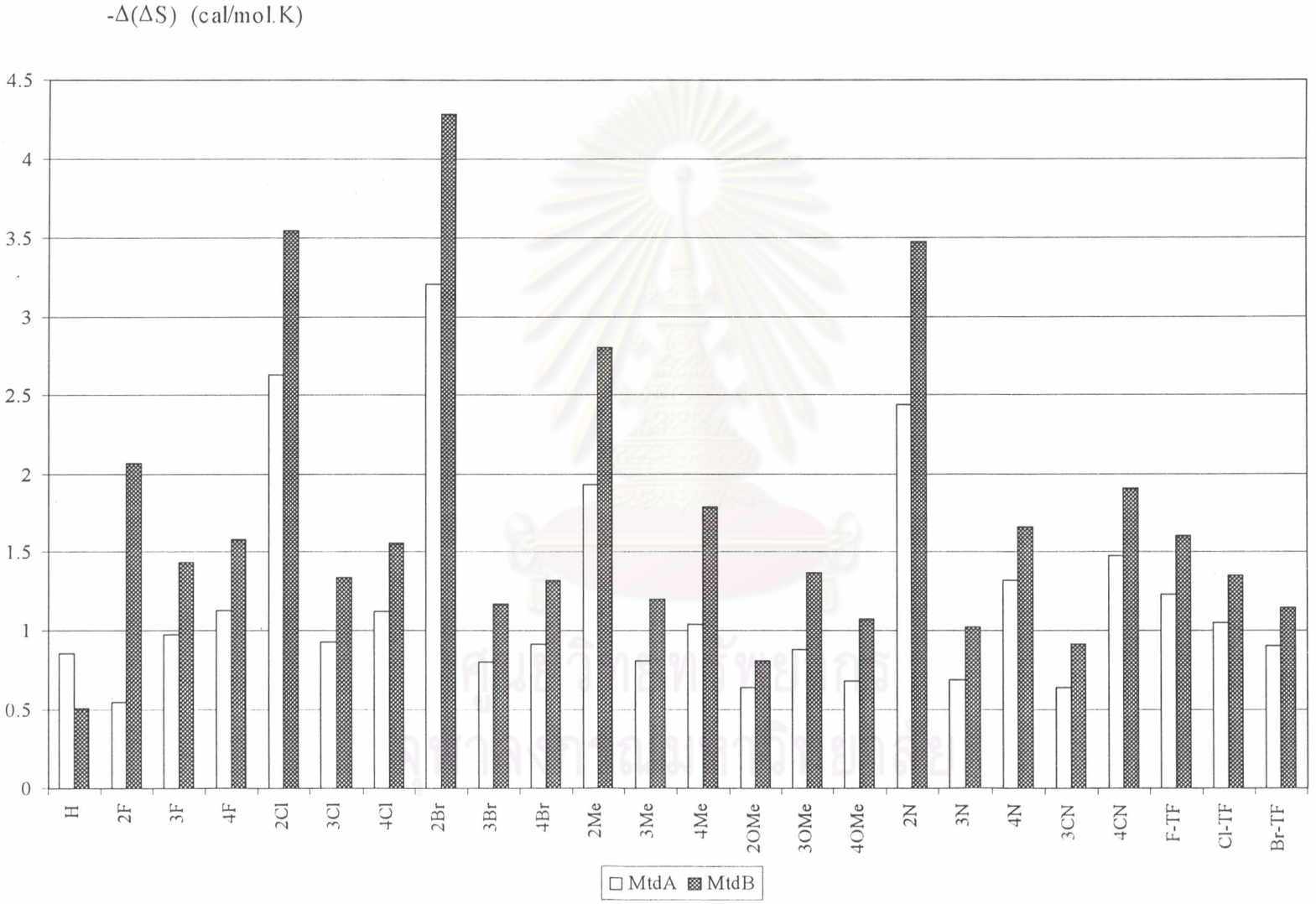

Figure 4.26 Comparison of entropy differences on BMe column calculated by two methods